ISSN 1070-3632, Russian Journal of General Chemistry, 2011, Vol. 81, No. 11, pp. 2222–2230. © Pleiades Publishing, Ltd., 2011.
Original Russian Text © A.A. Komlev, V.V. Gusarov, 2011, published in Zhurnal Obshchei Khimii, 2011, Vol. 81, No. 11, pp. 1769–1777.

Mechanism of the Nanocrystals Formation of the Spinel Structure in the $MgO–Al_2O_3–H_2O$ System under the Hydrothermal Conditions

A. A. Komlev[a] **and V. V. Gusarov**[a,b]

[a] *St. Petersburg State Technological Institute (Technical University),*
Moskovskii pr. 26, St. Petersburg, 190013 Russia
e-mail: brain86@bk.ru

[b] *Ioffe Physico-Technical Institute, Russian Academy of Sciences,*
Politekhnicheskaya ul. 26, St. Petersburg, 194021 Russia

Received April 28, 2011

Abstract—Using the method of hydrothermal synthesis,the nanoparticles of magnesium–aluminum spinel were obtained with a crystallite size of 40–50 nm. The sequence was determined of the chemical transformations under hydrothermal conditions of the initial magnesium–aluminum hydroxides obtained by co-precipitation, leading to the formation of nanoparticles $MgAl_2O_4$.

DOI: 10.1134/S1070363211110028

The phase relationships diagram for the system $MgO–Al_2O_3–H_2O$ built on the basis of the published data [1–7] (Fig. 1) shows that at low temperatures the products of reaction of the metal oxides with water are single and double hydroxides of magnesium and aluminum, and aluminum oxohydroxyde. With increasing temperature, these compounds decompose to form oxides. The magnesium and aluminum oxides form a single chemical compound, $MgAl_2O_4$. At elevated temperatures, the composition of this compound may deviate from the above stoichiometry, being enriched with magnesium oxide or aluminum oxide [3] (Fig. 1). The maximum deviation of the spinel phase composition from the stoichiometric ratio of oxides in the direction of enrichment of aluminum oxide to $MgAl_{2+\delta}O_{4+1.5\delta}$ corresponds to the value of $\delta = 0.85$ at $T = 1900°C$ [3]. One explanation for the spinel large nonstoichiometry at high temperatures can be given based on a comparison of the data on the thermodynamic properties of aluminum oxide with the structure corundum (α-Al_2O_3) and spinel structure (γ-Al_2O_3). Thermodynamic analysis of α-Al_2O_3 and γ-Al_2O_3 phases stability [8] suggests that when approaching the melting point the thermodynamic stability of phases based on Al_2O_3 with the corundum is reduced relative to the phase with the spinel structure, and the values of the Gibbs energy of these compounds near the melting temperature of aluminum oxide (T_m) become almost equal, that is, $\Delta G(\gamma\text{-}Al_2O_3 \rightarrow \alpha\text{-}Al_2O_3) = 0$ at $T \sim T_m$. In this case, the Gibbs energy of formation of phase of variable composition $MgAl_{2+\delta}O_{4+1.5\delta}$ from the $MgAl_2O_4$ and α-Al_2O_3 components is also significantly reduced with increasing temperature owing to decreasing the value of $\Delta G(\gamma\text{-}Al_2O_3 \rightarrow \alpha\text{-}Al_2O_3)$ and, as it can be concluded from the results of thermodynamic study of the formation of phases of variable composition [9], we can expect a substantial increase in the solubility of aluminum oxide in the phase based on $MgAl_2O_4$. In addition, due to the proximity of values of Gibbs energies of α-Al_2O_3 and γ-Al_2O_3 near the melting point of aluminum oxide [8], we can expect the stabilization of phase with the structure of γ-Al_2O_3 at the dissolving $MgAl_2O_4$ in it.

As can be seen from the data presented in [2, 4, 6, 8], for the Al_2O_3, AlOOH, and $Al(OH)_3$ is typical a variety of structural forms, which depends mainly on the synthesis conditions of these compounds and the presence in them of certain impurities. Despite the variety of structural forms of aluminum hydroxide and oxohydroxyde, they all have a layered structure (Table 1) [2, 5].

Table 1. Structure of layered hydroxides in the system of $MgO–Al_2O_3–H_2O$

Chemical compound	Structural form
$Mg(OH)_2$	**Brucite**. Layered structure. Each layer consists of two parallel, flat sheets, folded through the OH^- groups on the basis of the densest hexagonal packing, and Mg^{2+} ions located between the layers, occupying all the octahedral voids between the OH^- sheets.
$Al(OH)_3$	Layered structure. The layers of several distorted AlO_6 octahedra connected to each other by common edges. The Al atoms occupy two thirds of the octahedral voids of the slightly distorted close packing of O atoms. **α-$Al(OH)_3$ – Bayerite**. All O atoms occupy slightly distorted hexagonal close packing. **γ-$Al(OH)_3$ – Gibbsite**. The OH^- groups on the lower side of one layer lie directly above the OH^- groups of the layer below. **$Al(OH)_3$ – Nordstrandite**. Displacement of layers is intermediate between bayerite and gibbsite.
AlOOH	**α-AlOOH – Diaspore**. Hexagonal close packing of O atoms. The Al atoms are arranged in two layers of the occupied octahedral positions, alternating with two layers of unoccupied ones in both dense package and perpendicular directions. **γ-AlOOH – Boehmite**. The Al atoms are located in the centers of slightly distorted octahedra, O atoms occupy five vertices, and OH^- group occupies the sixth one. The octahedra are linked through common edges to form corrugated layers parallel to (010) plane.
$Mg_{1-x}Al_x(OH)_2(A^{n-})_{x/n}\cdot mH_2O$	**(x < 0.5): the** LDH of the **$Mg_6Al_2(OH)_{16}[A^{n-}]_m\cdot 4H_2O$** type, hydrotalcite structure. The layered brucite-like structure. The metal atoms are distributed statistically and occupy all octahedral positions. The water molecules and the (A^{n-}) groups are located in the intermediate layers. **(x > 0.5)**: the LDH of the **$MgAl_4(OH)_{12}[A^{n-}]_m\cdot x\ H_2O$** type. The layered gibbsite-like structure. Mg^{2+} cations occupy octahedral cavities in the gibbsite structure. The water molecules and the (A^{n-}) groups are located in the intermediate layers.

For MgO and $Mg(OH)_2$ is typical the stability of their structures regardless the impurity composition and the synthetic pre-history. The process of obtaining magnesium oxide and hydroxide is reflected only in the morphological characteristics of the formed phases [10–12].

In [1, 13–20] was shown that at the co-precipitation of magnesium and aluminum hydroxides occurs the formation of layered double hydroxides (LDH), of the chemical formula which can be written as $Mg_{1-x}\cdot Al_x(OH)_2(A^{n-})_{x/n}\cdot mH_2O$, where, A^{n-} is the interlayer anion, n is the anion charge, x is mole fraction, m is the number of H_2O molecules per formula unit contained in the interlayer (Fig. 2) [13, 17, 21]. The Mg^{2+}/Al^{3+} ratio can vary widely, and the magnitude of this relationship defines the LDH formation with the structure of hydrotalcite or gibbsite (Table 1).

The authors of [16, 18–20] give various ranges of x for the compounds $Mg_{1-x}Al_x(OH)_2(A^{n-})_{x/n}\cdot mH_2O$ of the hydrotalcite structure, which is derived from the structure of brucite $Mg(OH)_2$. According to [16, 20], this range is $0.17 < x < 0.33$, in other sources [18, 19] the range of variation of the x values is broader: $0.1 < x < 0.5$. In the brucite-like layers of hydrotalcite the metal atoms occupy statistically all octahedral positions [5]. Depending on the Mg^{2+}/Al^{3+} ratio, occurs substitution of the Mg^{2+} ions located in the centers of the octahedron by the Al^{3+} ions, which generates an uncompensated positive charge in the layer. The anions needed for the compensation of the charge are located in the interlayer space, which includes also water molecules (Fig. 2a) [13, 16–18, 21]. The unit cell contains four layers of hydrotalcite, with each fourth layer repeating the first layer location.

At higher proportion of Al^{3+} in the mixture of metal hydroxides precipitated together, along with the formation of hydrotalcite-like LDH is possible formation of hydroxides of complex composition, the structure of which, as pointed out in [7], is derived from the structure of bayerite α-$Al(OH)_3$. The compound of this type with the chemical formula corresponding to $MgAl_2(OH)_8$, is formed at a co-precipitation of the hydroxides at the ratio of $Mg^{2+}/Al^{3+} < 0.5$ [7]. The samples thus obtained are not single-phase, and along with $MgAl_2(OH)_8$ contain a number of hydrotalcite-like LDH and hydrated forms of aluminum oxide [7], depending on the Mg^{2+}/Al^{3+} ratio. In [22] was shown that $MgAl_2(OH)_8$ has a layered structure of brucite-bayerite type. Subsequent work on the synthesis and determination of the structure of complex hydroxides based on the structure of $[LiAl_2(OH)_6]_nX^{n-}$, showed that in contrast to all hydrotalcite-like compounds in which the layers are formed by a bivalent metal hydroxide, the structure-

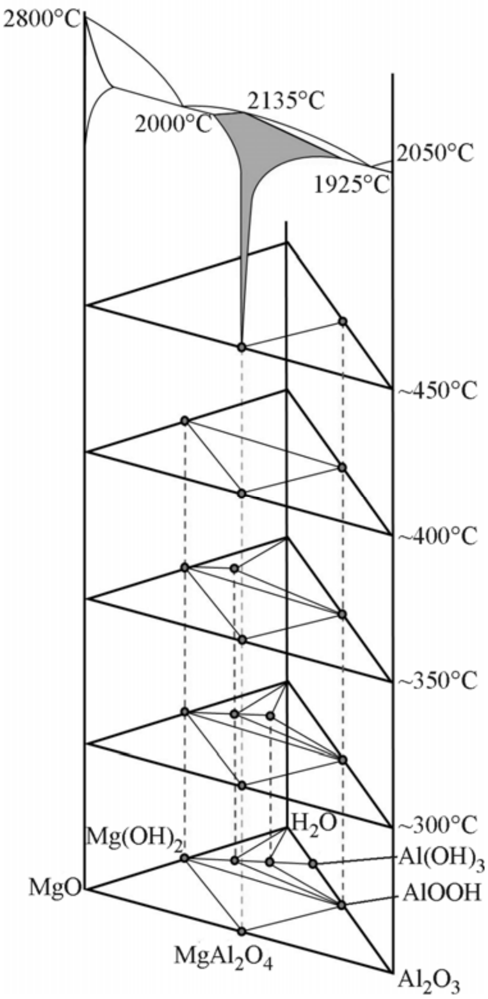

Fig. 1. Phase ratio diagram of the $MgO–Al_2O_3–H_2O$ system.

forming layers in these compounds are the layers of $Al(OH)_3$ [23–26]. In this case, the cations of lithium, as in the case of compound $MgAl_2(OH)_8$ cations of magnesium, are located in the third free octahedral layered cavities existing in the gibbsite layer (Fig. 2b). Thus, the hydroxides of similar composition can not be attributed to the group of the hydrotalcite-like LDH.

Comparing compounds $MgAl_2(OH)_8$ and $MgAl_2O_4$ in respect of Mg^{2+}/Al^{3+} ratio, is natural to assume that at the hydrothermal synthesis of magnesium–aluminum spinel is advisable to obtain in the step of the preparation of the initial compositions, the coprecipitation of hydroxides, a compound of the $MgAl_2(OH)_8$ composition, by the dehydroation of which in the area of the stability of spinel phase, apparently, can be obtained the compound $MgAl_2O_4$.

The issues concerning impact of the conditions of formation of double hydroxides on their structure and characteristics of chemical transformations at the dehydration were not considered in the literature. There are only the works indicating that such compounds have been obtained, or denoted to the determination of their structures [13–15, 19, 20, 22, 27, 28].

Of particular interest are the studies of the effect of phase formation processes on the structure of matter in the cases when the formed compounds are in a nanosized state [29–31]. In such cases potentially can form the compounds with a structure which is not typical for their existence. For example, as shown in [32], at a temperature of 200–300°C are formed the ZrO_2 nanocrystals in tetragonal or cubic forms, while at temperatures up to 1100°C the equilibrium modification of the zirconium dioxide is monoclinic [4, 6]. Also, the boundaries of isomorphous miscibility of components in the nanocrystals at low temperatures can be increased to the values characteristic of the high-temperature region, as observed, for example, for the $ZrO_2–In_2O_3$ solid solution [33, 34]. In the same study was found a decrease of the indium hydroxide dehydration temperature due to structural stabilization of its oxide at the formation of a solid solution $Zr_{1–x}In_xO_{2–0.5x}$, since zirconium hydroxide dehydration occurs at much lower temperatures than the dehydration of $In(OH)_3$ [3, 33].

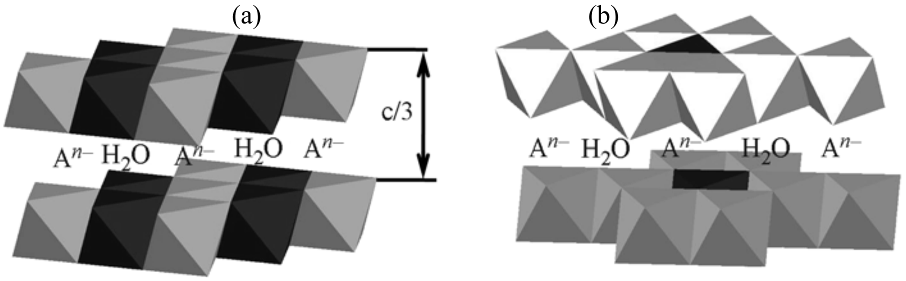

Fig. 2. Structure of layered double hydroxides $Mg_{1–x}Al_x(OH)_2(A^{n–})_{x/n}\cdot mH_2O$. (a) Hydrotalcite-like structure at $x < 0.5$. (Dark color) the positions of possible substitutions of the Mg^{2+} cations by Al^{3+} cations. (b) Hybbsite-like structure at $x > 0.5$. (Dark color) the positions of incorpotation Mg^{2+} cations in $Al(OH)_3$ lattice.

Table 2. The samples composition

Sample	$MgO:Al_2O_3$ ratio in the synthesis, mol %	$Mg^{2+}:Al^{3+}$ ratio in the synthesis, mol %	$MgO:Al_2O_3$ ratio, XRD data, mol %	$Mg^{2+}:Al^{3+}$ ratio, XRD data, mol %
MA1	50:50	1:2	43.9:56.1	1:2.56
MA2	40:60	1:3	37.2:62.8	1:3.38
MA3	30:70	1:4.67	29.9:70.1	1:4.70

In [35, 36] has been shown that the ZrO_2 nanoparticles included in the Al_2O_3 matrix can under certain conditions prevent the aluminum oxide crystallization, that is, they perform the function of a stabilizer of the amorphous state of the matrix material. Thus, it is relevant to study the effect of nanoscale spatial constraints on the structural features of the substances.

The formation mechanism and structure of the nanoparticles is affected also by the chemical and thermal history of the initial reaction system [37–39].

The contributions of the size factor, chemical and thermal history of the initial reaction composition, synthesis conditions, the presence of the impurity components of different composition to the formation of nanoparticles of a specific structure are very individual in each case, as shown by numerous studies [40–44]. Of particular interest is the study of the phase formation processes in the cases where the difference in the Gibbs energy of the formation of nanoparticles with different structures is negligible, since such a system is close to the neutral equilibrium [45], when the role of kinetic factors in the formation of nanoparticles of a certain structure can be decisive. In particular, to such systems can be assigned the system of $MgO–Al_2O_3–H_2O$ in a region enriched with aluminum oxide.

The possibility of formation of hydroxides of different structure and composition in the $MgO–Al_2O_3–H_2O$ system at the stage of precipitation of the oxides from the solutions of corresponding salts allows us potentially to study the effect of structural continuity between the precursors and the products of the dehydration reaction, the oxohydroxydes and oxides, respectively. The study of phase formation processes in the $MgO–Al_2O_3–H_2O$ system at the dehydration of the co-precipitated metal hydroxides is of interest, in particular, in the case of hydrothermal treatment of the original composition, since the typical for the hydrothermal synthesis increase in the number of variable parameters makes the study more informative.

To date, in the most studies on the phase formation in the $MgO–Al_2O_3–H_2O$ system is considered a relatively narrow range of variation in the Mg^{2+}/Al^{3+} ratio, and, as a rule, is studied the region of the compositions with predominance of the Mg^{2+} cation [13, 16, 19].

This work is aimed at the study of the formation of nanoparticles in the $MgO–Al_2O_3–H_2O$ system under hydrothermal conditions from the co-precipitated metal hydroxides, determination of the sequence of chemical transformations of the initially deposited compositions in supercritical conditions, the study of the influence of the chemical pre-history and the composition of the reaction mixture on the phase composition of the forming compounds.

Table 2 shows the composition of the samples obtained by co-precipitation. Along with the synthesis of stoichiometric spinel (sample Ma1), of great interest is to study the possibility of forming non-stoichiometric spinel $MgAl_{2+\delta}O_{4+1.5\delta}$ at the hydro-thermal dehydration of the corresponding LDH. In this regard, we obtained the source aluminum–magnesium hydroxides containing an excess of aluminum compared to the stoichiometric spinel (samples MA2 and MA3). On the basis of X-ray diffraction of these samples (Figs. 3–5) we can conclude that the crystalline phases in the complex hydroxide is only that with the structure of the $MgAl_2(OH)_8$ type.

After hydrothermal treatment of precipitates at 300°C under 500 atm ptessure occurs decomposition of $MgAl_2(OH)_8$ with the formation of hydrotalcite-type LDH with a layered structure of the $Mg_2Al(OH)_7$ and γ-AlOOH type (Figs. 3–5).

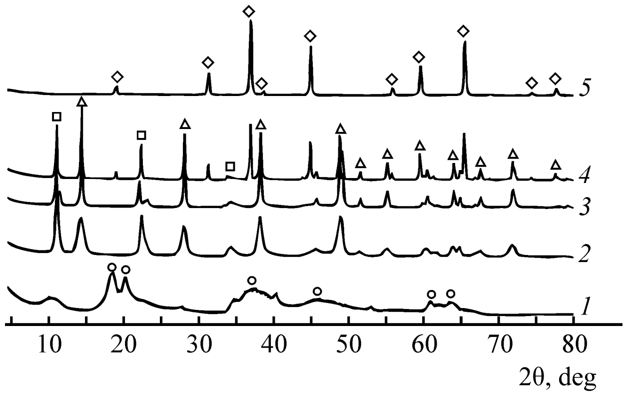

Fig. 3. X-ray diffraction pattern of MA1 sample in the initial state (*1*) and after hydrothermal treatment at 500 atm: (*2*) 300°C, (*3*) 350°C, (*4*) 400°C, and (*5*) 450°C.

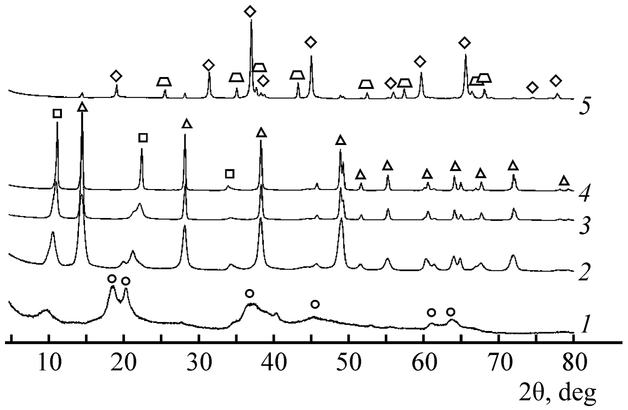

Fig. 4. X-ray diffraction pattern of MA2 sample in the initial state (*1*) and after hydrothermal treatment at 500 atm: (*2*) 300°C, (*3*) 350°C, (*4*) 400°C, and (*5*) 450°C.

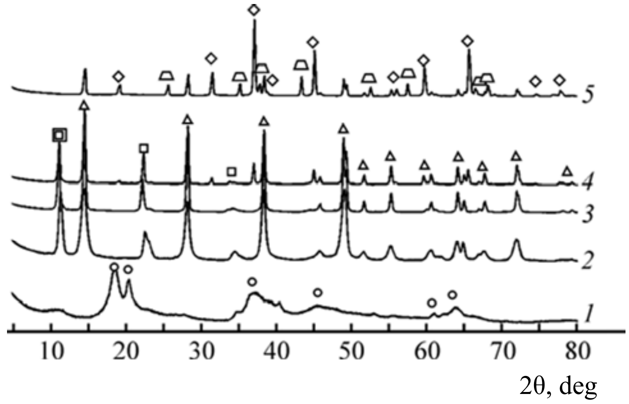

Fig. 5. X-ray diffraction pattern of MA3 sample in the initial state (*1*) and after hydrothermal treatment at 500 atm: (*2*) 300°C, (*3*) 350°C, (*4*) 400°C, and (*5*) 450°C.

$$MgAl_2(OH)_8 \rightarrow \text{hydrotalcite-type LDH} + AlOOH + H_2O. \quad (1)$$

The hydrotalcite-type LDH can be a hydroxide of the composition $Mg_{1-x}Al_x(OH)_2(A^{n-})_{x/n}{\cdot}mH_2O$ ($x < 0.5$). The anions compensating the positive charge of the brusite-like layers can be the the ions NO_3^- and OH^-: $Mg_2Al(OH)_{7-x}(NO_3)_x$ [7]. In the LDH, as a result of intercalation of the NO_3^- ions, the interlayer distance may be considerably higher than in brucite. As shown in [16, 46], the introduction of ions in the interlayer space may lead to an increase in the LDH unit cell *c* parameter reflected by shifts of the peaks in the diffraction patterns (Figs. 3–5, curves *2*, *3, 4*).

The reason for the formation of LDH of the $Mg_2Al(OH)_7$ type at the hydrothermal treatment at elevated temperature can apparently be explained by the similarity of its structure with the structure of brucite, which is the most thermally stable hydroxide in the $Al(OH)_3$–$Mg(OH)_2$ section (Fig. 1). In addition, there is an information about the high thermodynamic stability of hydrotalcite-like LDH [47].

The decomposition reaction (1) results in the formation of γ-AlOOH, which under the reaction conditions corresponds to the equilibrium state (Fig. 1). When the hydrothermal treatment is carried out at a higher temperature, the particles of all forms of hydrated oxides grow in size, as evidenced by the narrowing of the reflections in the diffraction patterns (Figs. 3–5). Increase in the synthesis temperature to 350°C does not results in changes in the phase composition of the powders. A difference is observed when temperature reaches 400°C ($P = 500$ atm). With these parameters of hydrothermal synthesis is formed a phase of magnesium–aluminum spinel. Note that the temperature of the $MgAl_2O_4$ formation from the co-precipitated hydroxides at the thermal treatment in air, that was experimentally determined in [23, 24], is higher than required in the conditions of the hydrothermal synthesis. At the temperature exceeding 350°C, the LDH of the $Mg_2Al(OH)_7$ type loses its stability (see Fig. 1) making possible the proceeding of several reactions leading to the formation of $MgAl_2O_4$. First of all, a direct interaction of $Mg_2Al(OH)_7$ with the aluminum oxohydroxyde formed in the stage of $MgAl_2(OH)_8$ decomposition is possible [reaction (1)], which results in the synthesis of magnesium–aluminum spinel [reaction (2)]:

$$Mg_2Al(OH)_7 + 3AlOOH \rightarrow 2MgAl_2O_4 + 5H_2O. \quad (2)$$

Another pathway of the formation of magnesium–aluminum spinel can be represented as a sequence of the transformations:

$$Mg_2Al(OH)_7 \rightarrow 2Mg(OH)_2 + AlOOH + H_2O, \quad (3)$$

$$Mg(OH)_2 + 2AlOOH \rightarrow MgAl_2O_4 + 2H_2O. \quad (4)$$

Presumably, in the both [reactions (2), (4)] transformations the γ-AlOOH can be a nucleation point for the formation of $MgAl_2O_4$, because γ-AlOOH is similar by structure with the shpinel-like γ-Al_2O_3 [2, 4], being its structural precursor at the dehydration.

Summing up the reactions (1)–(4), the formation of magnesium–aluminum spinel from the initial hydroxide $MgAl_2(OH)_8$ can formally be written as [reaction (5)]:

$$MgAl_2(OH)_8 \rightarrow MgAl_2O_4 + 4H_2O. \quad (5)$$

But studies showed that $MgAl_2(OH)_8$ does not transform immediately to $MgAl_2O_4$ in the dehydration reaction (5). Apparently, the decisive factor in the formation of spinel $MgAl_2O_4$ from $MgAl_2(OH)_8$ is not the similarity of the Mg^{2+}/Al^{3+} component ratio in these compounds, but structural similarity of the more thermodynamically stable phases $Mg_2Al(OH)_7$ and γ-AlOOH with the parent compound $MgAl_2(OH)_8$. The structural similarity of the initial and intermediate compounds leads to the fact that the reaction (1) proceeds at a high rate [48], separating spatially the formed therewith precursors of $Mg_2Al(OH)_7$ and γ-AlOOH. Formation of the $MgAl_2O_4$ spinel, which occurs at a higher temperature than occurs the $MgAl_2(OH)_8$ dehydration (Fig. 1) and therefore proceeds with the separation of the reactions (1) and (2)–(4) by the temperature fields may proceed in these conditions as a multistep process only.

The direct formation of $MgAl_2O_4$ in the dehydration of $MgAl_2(OH)_8$ could be realized, apparently, either in the case of stability of the hydroxide below the temperature of the $MgAl_2O_4$ formation (that is, below 400°C) or when the rate of the temperature increase in the reaction system up to the temperature at which the dehydration of $MgAl_2(OH)_8$ along the reaction (5) becomes possible (relating to the conditions of hydrothermal treatment, this temperature corresponds to ~400°C at a pressure of about 500 atm) and the rate of the reaction (5) exceed significantly the rate of reaction (1). Note that carying out the synthesis in such a regime it could be, apparently, possible to perform the synthesis of non-stoichiometric spinel containing Al_2O_3 in excess. Figure 6 shows schematically the possible ways of chemical transformations of the original double hydroxides with the structure of the $MgAl_2(OH)_8$ type at the hydrothermal dehydration.

The chemical transformations (1)–(5) describe only the region of formation of stoichiometric spinel and do not account for the excess of the aluminum-containing component that exists in the samples MA2 and MA3. The chemical reactions at the hydrothermal dehydration of these samples may differ from the dehydration of $MgAl_2(OH)_8$, either in the formation of non-stoichiometric spinel $MgAl_{2+\delta}O_{4+1.5\delta}$, or in the formation, along with the stoichiometric spinel $MgAl_2O_4$, of addition phases on the basis of γ-AlOOH or α-Al_2O_3, in correspondence with the equilibrium conditions at corresponding temperatures (Fig. 1). Experimental results show that dehydration under the hydrothermal conditions of co-precipitated magnesium and aluminum hydroxides at a ratio of $Mg^{2+}/Al^{3+} \leq 1/3$ (Table 2) leads to a mixture of phases (Figs. 4 and 5). Hydrothermal treatment of the samples MA2 and MA3 at a high temperature (T = 400, 450°C, P = 500 atm) leads to formation in the corresponding compositions of $MgAl_2O_4$ and α-Al_2O_3, which is fully consistent with the diagram of the equilibrium phase relations in the $MgO–Al_2O_3–H_2O$ system (Fig. 1). The crystallite size (coherent scattering areas) of the phases formed calculated by the Scherrer formula [49] from the width of the diffraction peaks (Figs. 3–5) is 40–50 nm for $MgAl_2O_4$ and 55–60 nm for α-Al_2O_3.

The results obtained show that in the samples of MA2 and MA3, as well as in the sample of MA1, magnesium–aluminum spinel is synthesized from the co-precipitated magnesium and aluminum hydroxides through the formation of several intermediates (Figs. 4, 5). The original double hydroxide with the structure of $MgAl_2(OH)_8$ type formed at the co-precipitation decomposes under hydrothermal conditions to form a structurally close hydrotalcite-like LDH and aluminum oxohydroxyde, which eventually are precursors in the formation of the spinel phase (Fig. 6). Direct transfer of the precipitated source compound into the phase of the magnesium–aluminum spinel with maintaining the predetermined ratio of the Mg^{2+} and Al^{3+} cations does not occur under the studied hydrothermal conditions, as follows from the X-ray diffraction data (Figs. 4, 5). As in the case of hydrothermal treatment of the source MA1 sample, this is caused apparently by the existence in the $MgO–Al_2O_3–H_2O$ system of the hydroxides similar in structure to the original LDH and, therefore, formed with a high rate at the decomposition of the

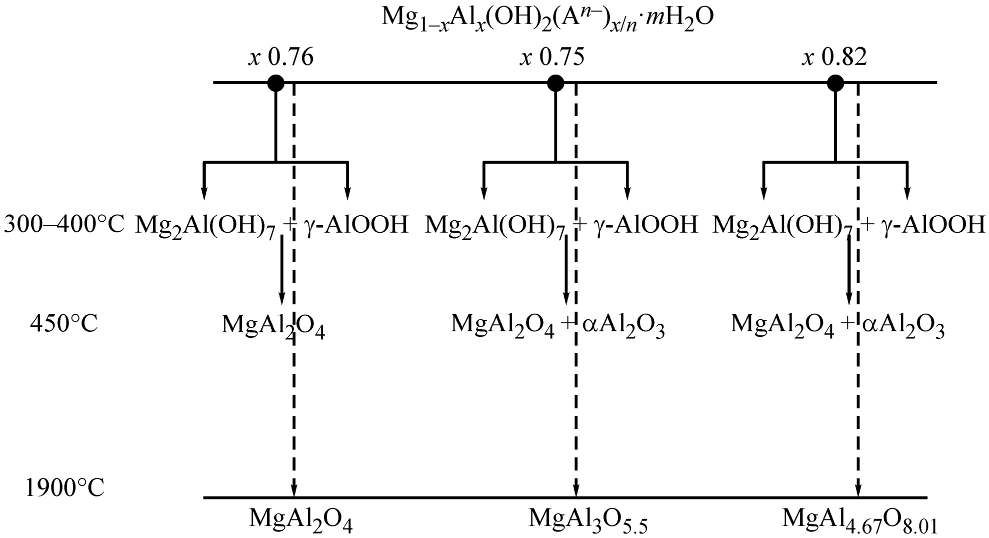

Fig. 6. Scheme of the possible chemical transformations at the dehydration of the LDH of $MgAl_2(OH)_8$ type under hydrothermal conditions.

starting material [48], which differ in the stoichiometry from the composition of the synthesized spinel phase $MgAl_{2+\delta}O_{4+1.5\delta}$. In this regard, the spinel formation from the intermediates can occur only through a step of mass transfer of the components from one phase to another, that is, rather slowly. In such circumstances, as a rule, are formed only equilibrium products, including in particular the stoichiometric spinel $MgAl_2O_4$ at the considered temperature of the synthesis, 400°C (Fig. 1). The nonstoichiometric spinel $MgAl_{2+\delta}O_{4+1.5\delta}$ can not form along the described mechanism of the process of dehydration of the initial composition (Fig. 6) in the temperature range of existence of the equilibrium $MgAl_2O_4$.

Comparing the mechanism of formation of nanocrystals of $MgAl_2O_4$ proposed in this paper with the results of [6, 50, 51] on the formation of nanocrystals of ZrO_2 and Al_2O_3, one can conclude that apparently the reason for the formation of nanoparticles in the structural forms that are non-equilibrium in relation to the structure of the macro particles is, first of all, the genetic continuity of the initial materials and the structures of the formed from them nano-sized nuclei of a new phase.

Thus, we can conclude that while in the case of genetic structural continuity of the parent and formed nanoparticles the phase formation occurs at a high rate and formation of the non-equilibrium phases is possible in these conditions, the nanoparticles are formed from spatially separated reactants, the process of phase formation slows, and the final product composition and structure correspond to the equilibrium state.

EXPERIMENTAL

Samples were prepared by precipitation with ammonium hydroxide of magnesium and aluminum hydroxides from the solutions of corresponding nitrates. The following initial substances were used: $Mg(NO_3)_2\cdot 6H_2O$ (GOST 11088-75), $Al(NO_3)_3\cdot 9H_2O$ (GOST 3757-75), 25% solution of NH_4OH (GOST 24147-80), distilled water (GOST 6709-72). The co-precipitation was carried out by adding a solution of ammonium hydroxide to a solution of metal salts. For the study were selected compositions with the different molar ratio of magnesium and aluminum cations. The ratios recalculated on the MgO/Al_2O_3 oxides were 50:50, 40:60, and 30:70 mol %. These ratios were selected on the basis of the data on the range of non-stoichiometric compositions of magnesium–aluminum spinel (Fig. 1).

The suspension of co-precipitated hydroxide was filtered and washed till the absence of ammonium and nitrate ions in the filtrate. The precipitates were dried at 60°C for 48 h. Hydrothermal processing of samples was carried out in the temperature range 300–450°C in 50°C steps at a pressure of 500 atm for 4 h.

The elemental composition of samples was determined by X-ray spectral microanalysis on a scanning electron microscope Hitachi S-570 with a Bruker Quantax 200 microanalysis system.

The phase composition of the samples was determined by X-ray diffraction (XRD) using a Shimadzu X-ray diffractometer XRD-7000, CuK_{α}-radiation ($\lambda = 0.154051$ nm.). Registering was carried out in the range of 2θ angles from 4° to 80°.

The size of the crystallites was calculated using the Scherrer formula [49] from the broadening of the X-ray diffraction peaks of the samples.

ACKNOWLEDGMENTS

This work was financially supported by the Government of St. Petersburg, the Russian Foundation for Basic Research (grant no. 10-03-00 889-a) and the Ministry of Education and Science under the Federal Target Program "Research and development of the priority directions of scientific-technological complex of Russia for 2007–2012 years," the State Contract no. 16.516.11.6073.

REFERENCES

1. Chalyi, V.P., *Gydrookisi metallov* (Metal Hydroxides), Kiev: Naukova Dumka, 1972, p. 163.
2. Wells, A.F., *Structural Inorganic Chemistry*, vol. 2, Moscow: Mir, 1987, p. 696.
3. Toropov, N.A., Barzakovskii, V.P., Lapin, V.V., and Kurtseva, N.N., *Diagrammy sostoyaniya silikatnykh sistem. Spravochnik. Vypusk pervyi. Dvoinye sitemy* (State Diagrams of Silicate Systems. Handbook. First Issue. Dual Systems), Leningrad: Nauka, 1969, p. 822.
4. Toropov, N.A., Barzakovskii, V.P., Bondar', I.A. and Udalov, Yu.P., *Diagrammy sostoyaniya silikatnykh sistem. Spravochnik. Vypusk vtoroi. Metall-kislorodnye soedineniya silikatnykh sistem* (State Diagrams of Silicate Systems. Handbook. Second Issue. Metal-Oxygen Compounds of the Silicate Systems) Leningrad: Nauka, 1969, p. 372.
5. *Mineraly. Spravochnik* (Minerals. Handbook), Chukhrov, F.V. and Bonshtedt-Kupletskaya, E.M., Eds., vol. 11, no. 3, Moscow: Nauka 1967, p. 676.
6. Al'myasheva, O.V., *Candidate Sci. (Chem.) Dissertation,* St. Petersburg, 2007.
7. Ivanova, A.S., Dzis'ko, V.A., and Ketchik, S.V., *Zh. Neorg. Khim*., 1980. vol. 25, no. 9, p. 2330.
8. Ishutina, Zh.N., *Candidate Sci. (Chem.) Dissertation*, St. Petersburg, 1997.
9. Suvorov, S.A., Semin, E.G., and Gusarov, V.V., *Fazovye diagrammy i termodinamika oxydnykh tverdykh rastvorov* (Phase Diagrams and Thermodynamics of Oxide Solid Solutions), Leningrad: Leningrad. Gos. Univ., 1986.
10. Xu, B., Deng, H., Dai, Y., and Yang, B., *Trans. Nonferrous Met. Soc. China*, 2007, vol. 17, p. 671.
11. Hsu, J.P. and Nacu, A., *Colloid and Surfaces A: Physicochem. Eng. Aspects*, 2005, vol. 262, p. 220.
12. Wei, Q. and Lieber, C.M., *Mat. Res. Soc. Symp. Proc.*, 2000, vol. 581, p. 3.
13. Yang, Q.Z., Zhang, C.G., Sun, D.J., and Jin, Z.L., *Chinese Chem. Lett*., 2003, vol. 14, no. 1, p. 79.
14. Tomilov, N.P. and Devyatkina, E.T., *Neorg. Mater*., 1990, vol. 26, no. 12, p. 2556.
15. Dzis'ko, V.A., Ivanova, A.S., Plyasova, L.M., and Ketchik, S.V., *Izv. Akad. Nauk SSSR. Ser. Khim. Nauk*, 1978, no. 5, p. 983.
16. Kovanda, F., Jindova, E., and Dousova, B., *Acta Geodyn. Geomater*., 2009, vol. 6, no. 1, p. 111.
17. Aramendia, M., Aviles, Y., Borau, V., Luque, J., Marinas, J., Ruiz, J., and Urbano, F., *J. Materials Chem*., 1999, vol. 9, p. 1603.
18. Gabrovska, M., Edreva-Kardjieva, R., Angelov, V., Crisan, D., Munteanu, G., and Vrdine, J., *Revue Roumaine de Chimie*, 2007, vol. 52, no. 5, p. 521.
19. Lee, J., Liu, Y., and Liu, X., *J. Applied Science in Enviromental Sanitation*, 2010, vol. 5, no. 4, p. 345.
20. Xu, X., Li, D., Song, J., Lin, Y., Lv, Z., Wei, M., and Duan, X., *Particuology*, 2010, vol. 8, no. 3, p. 198.
21. Costa, F.R., *Erlangung des ak. Grades Dr.-Ing. Diss*., Dresden, 2007.
22. Ketchik, S.V., Plyasova, L.M., and Ivanova, A.S., *Neorg. Mater*., 1980. vol. 16, no. 11, p. 1978.
23. Starikova, E.V., *Candidate Sci. (Chem.) Dissertation*, Moscow, 2007.
24. Isupov, V.P., Chupakhina, L.E., Mitrofanova, R.P., and Tarasov, K.A., *Khimiya v Interesakh Ustoichivogo Razvitiya*, 2000, nos. 1–2, p. 121.
25. Kozlova, S.G., Gabuda, S.P., Isupov, V.P., and Chupakhina, L.E., *Zh. Strukt. Khim*., 2003. vol. 44, no. 2, p. 228.
26. Menzheres, L., T., Kotsupalo, N.P., and Mamylova, E.V., *Journal of Materials Synthesis and Processing*, 1999, vol. 7, no. 4, p. 239.
27. Ledovskaya, E.G., Gobelkov, S.V., Litvinenko, L.N., Logvinkov, D.S., Mironova, A.G., Odeichuk, M.A., Poltavtsev, N.S., and Tarasov, R.V., *Voprosy Atomnoi Nauki i Tekhniki*, 2006, no. 1, p. 160.
28. Gobelkov, S.V., Tarasov, R.V., Poltavtsev, N.S., Kurilo, Yu.P., Starolat, M.P., Andrievskaya, N.F., Mironova, A.G., Ledovskaya, E.G., Litvinenko, L.N., and Belkin, F.V., *Neorg. Mater*., 2007, vol. 43, no. 4, p. 462.

29. Tret'yakov, Yu.D., Lukashin, A.V., and Eliseev, A.A., *Usp. Khim.*, 2004, vol. 73, no. 9, p. 974.
30. Suzdalev, I.P., *Usp. Khim.*, 2009, vol. 78, no. 3, p. 266.
31. Al'myasheva, O.V., Vlasov, E.A., Khabenskii, V.B., and Gusarov, V.V., *Zh. Prikl. Khim.*, 2009, vol. 82, no. 2, p. 224.
32. Pozhidaeva, O.V., Korytkova, E.N., Romanov, D.P., and Gusarov, V.V., *Zh. Obshch. Khim.*, 2002, vol. 72, no. 6, p. 910.
33. Artamonova, O.V., Al'myasheva, O.V., Mittova, I.Ya., and Gusarov, V.V., *Neorg. Mater.*, 2006, vol. 42, no. 10, p. 1072.
34. Artamonova, O.V., Al'myasheva, O.V., Mittova, I.Ya., Lavrushina, S.S., and Gusarov, V.V., *Fiz. Khim. Stekla*, 2005, vol. 31, no. 2, p. 318.
35. Al'myasheva, O.V. and Gusarov, V.V., *Dokl. Akad. Nauk*, 2009, vol. 424, no. 5, p. 641.
36. Al'myasheva, O.V. and Gusarov, V.V., *Zh. Neorg. Khim.*, 2007, vol. 52, no. 8, p. 1194.
37. Galkin, A.A. and Lunin, V.V., *Usp. Khim.*, 2005, vol. 74, no. 1, p. 24.
38. Zyryanov, V.V., *Usp. Khim.*, 2008, vol. 77, no. 2, p. 107.
39. Vanetsev, A.S. and Tret'yakov, Yu.D., *Usp. Khim.*, 2007, vol. 76, no. 5, p. 435.
40. Al'myasheva, O.V., Fedorov, B.A., Smirnov, A.V., and Gusarov, V.V., *Nanosistemy. Fizika, Khimiya, Matematika*, 2010, vol. 1, no. 1, p. 26.
41. Mishra, V.V., Garg, A.K., and Agrawal, D.C., *Bull. Mater. Sci.*, 1998 , vol. 21, no. 1, p. 81.
42. Li, H., Liang, K., Gu, S., and Xiao G., *J. Mater. Sci. Lett.,* 2001, vol. 20, p. 1301.
43. Goldstein, A. and Giefman, L., Bar Ziv, S., *J. Mater. Sci. Lett.*, 1998, vol. 17, p. 977.
44. Thanabodeekij, N., Sathupunya, M., Jamieson, A.M., and Wongkasemjit, S., *Materials Characterization*, 2003, vol. 50, p. 325.
45. Gusarov, V.V., Abstract of Papers, *15th Int. Conf. on Chemical Thermodynamics in Russia*, 2005, Moscow, vol. I, p. 26.
46. Raki, L., Beaudoin, J.J., and Mitchel, L., *Cement and Concrete Research*, 2004, vol. 34, no. 9, p. 1717.
47. Duan, X. and Evans, D.G., *Structure and Bonding*, 2005, vol. 117, p. 234.
48. Gusarov, V.V., *Zh. Obshch. Khim.*, 1997, vol. 67, no. 12, p. 1959.
49. Rusakov, A.A., *Rentgenografiya metallov* (X-Ray Diffraction of Metals), Moscow: Atomizdat, 1977, p. 480.
50. Sharikov, F.Yu., Al'myasheva, O.V., and Gusarov, V.V., *Zh. Neorg. Khim.*, 2006, vol. 51, no. 10, p. 1538.
51. Al'myasheva, O.V., Korytkova, E.N., Maslov, A.V., and Gusarov, V.V., *Neorg. Mater.*, 2005, vol. 41, no. 5, p. 540.